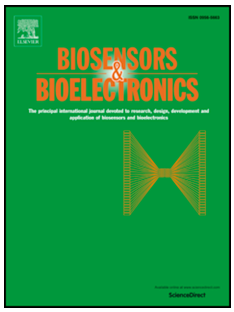

AI-assisted Smartphone-based Colorimetric Biosensor for Visualized, Rapid and Sensitive Detection of Pathogenic Bacteria

Rongwei Cui, Huijing Tang, Qing Huang, Tingsong Ye, Jiyang Chen, Yinshen Huang, Chongchao Hou, Sihua Wang, Sami Ramadan, Bing Li, Yunsheng Xu, Lizhou Xu, Danyang Li

PII: S0956-5663(24)00374-9

DOI: https://doi.org/10.1016/j.bios.2024.116369

Reference: BIOS 116369

To appear in: *Biosensors and Bioelectronics*

Received Date: 2 March 2024

Revised Date: 2 May 2024

Accepted Date: 4 May 2024

Please cite this article as: Cui, R., Tang, H., Huang, Q., Ye, T., Chen, J., Huang, Y., Hou, C., Wang, S., Ramadan, S., Li, B., Xu, Y., Xu, L., Li, D., AI-assisted Smartphone-based Colorimetric Biosensor for Visualized, Rapid and Sensitive Detection of Pathogenic Bacteria, *Biosensors and Bioelectronics*, https://doi.org/10.1016/j.bios.2024.116369.

AI-assisted Smartphone-based Colorimetric Biosensor for Visualized, Rapid and Sensitive Detection of Pathogenic Bacteria

Rongwei Cui[a], Huijing Tang[a], Qing Huang[a], Tingsong Ye[a], Jiyang Chen[c], Yinshen Huang[c], Chongchao Hou[a], Sihua Wang[a], Sami Ramadan[d], Bing Li[e], Yunsheng Xu[a,f], Lizhou Xu[b]*, Danyang Li[a,f]*

a Research Center, The Seventh Affiliated Hospital, Sun Yat-sen University, Shenzhen 518107, China

b ZJU-Hangzhou Global Scientific and Technological Innovation Center, Zhejiang University, Hangzhou 311215, China

c School of Biomedical Engineering, Sun Yat-sen University, Shenzhen 518107, China

d Department of Materials, Imperial College London, London SW7 2AZ, UK

e Institute for Materials Discovery, Department of Chemistry, University College London, London WC1E 7JE, UK

f Shenzhen Key Laboratory of Chinese Medicine Active Substance Screening and Translational Research, Shenzhen 518107, China

Corresponding authors:

Dr Lizhou Xu: lzxu@zju.edu.cn

Dr Danyang Li: lidy55@mail.sysu.edu.cn

Abstract

Accurate and effective detection is essential to against bacterial infection and contamination. Novel biosensors, which detect bacterial bioproducts and convert them into measurable signals, are attracting attention. We developed an artificial intelligence (AI)-assisted smartphone-based colorimetric biosensor for the visualized, rapid, sensitive detection of pathogenic bacteria by measuring the bacteria secreted hyaluronidase (HAase). The biosensor consists of the chlorophenol red-β-D-galactopyranoside (CPRG)-loaded hyaluronic acid (HA) hydrogel as the bioreactor and the β-galactosidase (β-gal)-loaded agar hydrogel as the signal generator. The HAase degrades the bioreactor and subsequently determines the release of CPRG, which could further react with β-gal to generate signal colors. The self-developed YOLOv5 algorithm was utilized to analyze the signal colors acquired by smartphone. The biosensor can provide a report within 60 mins with an ultra-low limit of detection (LoD)

of 10 CFU/mL and differentiate between gram-positive (G+) and gram-negative (G-) bacteria. The proposed biosensor was successfully applied in various areas, especially the evaluation of infections in clinical samples with 100% sensitivity. We believe the designed biosensor has the potential to represent a new paradigm of "ASSURED" bacterial detection, applicable for broad biomedical uses.

Keywords

Bacteria detection; Hyaluronidase; Colorimetric biosensor; Smartphone; YOLOv5

1. Introduction

Pathogenic bacterial contamination in food and environment significantly threatens global health and economic stability (Nißler *et al.* 2020). The World Health Organization (WHO) estimates that 600 million people are infected by pathogenic bacteria, resulting in 420,000 deaths worldwide per year. Antibiotics are commonly prescribed for bacterial infection (Gui *et al.* 2023). However, given the significant increase in antimicrobial resistance, empirical treatment may not always be effective as the clinical microbiology laboratories may not be able to provide reports quickly enough in many cases (Mi *et al.* 2022).

The culture method has represented the gold standard in bacteria detection (Dsouza *et al.* 2022). However, growing bacteria in laboratory conditions is not a sensitive and efficient method. Assays that rely on the recognition between biomolecules such as polymerase chain reaction (PCR) and enzyme-linked immunoassays (ELISAs), are considered reliable in accurately identifying bacterial strains (Xu *et al.* 2021). However, the limitations of those methods include their complexity, high cost and requirement of professional operation. Novel biosensors based on changes in electrochemical properties (such as impedance, amperometry and voltammetry) after the diagnosis of bacteria, offer portability, fast responses and adequate sensitivity (Liu *et al.* 2023; Zhang *et al.* 2023). However, these biosensors suffer from false positives. Thus, there is an urgent need to develop biosensors that satisfy the WHO's "ASSURED" criteria, that is, affordable, sensitive, specific, user-friendly, rapid and robust, equipment-free, and deliverable to end users (Petrucci *et al.* 2021).

Many extracellular products of pathogenic bacteria have tissue-damaging effects (Rentzsch *et al.* 2020). Among these, HAase, as bacterial spreading factors, enables the degradation of substrate hyaluronate (for example, HA) in the extracellular matrix and facilitating the invasion of host tissues (Zamboni *et al.* 2023). A considerable number of studies have demonstrated that the aspects of the production of HAase are associated with the type of bacteria (Shenashen *et al.* 2022). For instance, G+ are generally known to produce a higher amount of HAase compared to G-, making HAase a potential biomarker in distinguishing between G+ and G- (Mohammed *et al.* 2022). The detection of the HAase of bacteria also has distinct advantages, such as improved

specificity and simplified sample handling process, compared to other physicochemical indicators (Mohammed *et al.* 2022). Previous HAase-based bacteria detection studies electrically monitored the steric/electrostatic nanochannels, which were blocked by the formation of an antibody-HAase complex (Creran *et al.* 2014). However, the signal transmission process and data analysis involved are complicated and time-consuming. Therefore, simpler and smarter result acquisition and analysis method would be preferable to meet the "ASSURED" criteria.

Among all readout forms, the visualization method is particularly convenient and intuitively satisfactory (AbdElFatah *et al.* 2023). Meanwhile, machine learning, as a key technique of artificial intelligence (AI), is becoming a popular method to ensure the high efficiency and accuracy of data analysis (Meng *et al.* 2022). Various algorithms have been reported with regard to the analysis of color-based results, such as the convolutional neural network (CNN), support vector machine (SVM), open computer vision library (OpenCV) and you only look once (YOLO) (Flachot and Gegenfurtner 2021). Among them, YOLO could reduce the computational complexity with the desired accuracy (Chen *et al.* 2023a). However, methods using machine learning to analyze the colorimetric results of bacterial detection have not yet been reported.

In this study, an AI-assisted smartphone based colorimetric biosensor was developed for the visualized, rapid, and sensitive detection of pathogenic bacteria using secreted HAase as the target. The biosensor design is shown in Scheme 1. It consists of the CPRG-loaded HA hydrogel as the bioreactor and the β-gal-loaded agar hydrogel as the signal generator. The bacterial HAase first degrades the bioreactor in a concentration-dependent manner and subsequently influencing the release of CPRG, which can further react with β-gal immobilized in agar hydrogel, to generate different colors. We then utilized smartphone to capture the colors and correlate them with the initial bacteria concentration using a self-developed YOLOv5 algorithm. The developed biosensor can provide a report in 60 mins using a simple and user-friendly detection process and achieves an ultra-low LoD of 10 CFU/mL of bacteria. We confirmed the superior performance of the biosensor in detecting bacteria in food samples, performing antimicrobial susceptibility testing and assessing bacterial infection in clinical cases. The developed biosensor has the potential of leading a new paradigm of "ASSURED"

bacterial detection and is applicable in a broad range of biomedical uses.

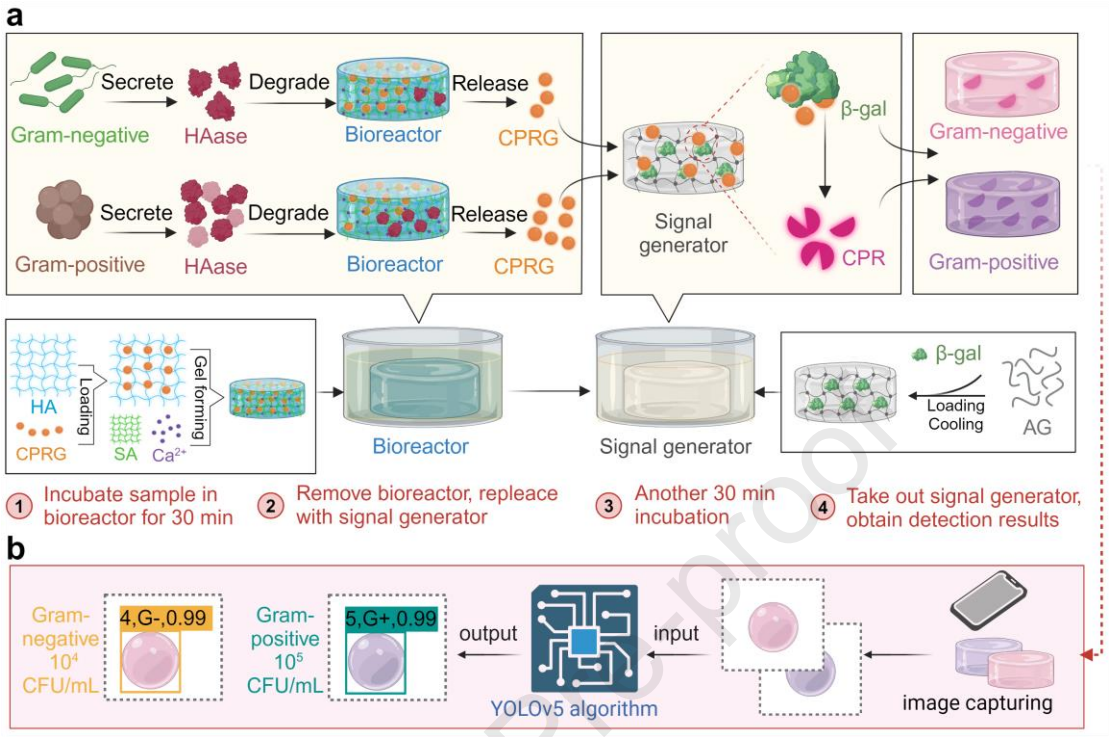

Scheme 1. Illustration of the AI-assisted smartphone-based colorimetric biosensor composed of HA hydrogel bioreactor and agar hydrogel signal generator. (**a**) Schematic diagram of the colorimetric detection of bacteria type and concentration, where the insets illustrate the preparation of bioreactor and signal generator. (**b**) Acquisition and analysis of the detection results using the YOLOv5 algorithm.

2. Results and Discussion

2.1 Characterization and Optimization of the Biosensor

2.1.1 Optimization of the Color Reaction between CPRG and β-gal

CPRG is a long-wavelength yellow substrate which could be hydrolyzed by β-gal to produce chlorophenol red (Creran *et al.* 2014). The color reaction between different concentrations of CPRG (0-1000 μg/mL) and β-gal (0-100 μg/mL) was first investigated. As described in Fig. 1a, all reactions are initially yellow (the color of CPRG), and at intermediate enzyme/substrate concentrations, the reaction color varies from shades of yellow, orange, red, and purple. The UV-vis spectra (Fig. 1b) indicated that the characteristic absorption peak of CPRG at 410 nm gradually disappeared with the addition of β-gal along with the emergence of a new absorption peak at 570 nm. When the concentration of β-gal was 20 μg/mL or above, the color of the reaction was

solely dependent on the concentration of CPRG, thus β-gal at 20 μg/mL was used as an optimal concentration for the preparation of signal generator hydrogel.

2.1.2 Evaluation of HAase Productivity of Different Bacteria

HAase productivity of various bacteria (*E. coli*, *P. aeruginosa*, *S. aureus* and Group A *streptococcus* (GAS)) was validated. As shown in Fig. 1c, the concentration of HAase secreted by those four representative strains linearly correlated with the concentration of bacteria ($R^2 > 0.99$). Interestingly, we found that the G- (*E. coli* and *P. aeruginosa*) had HAase productivity in the range of 0.2-3.4 mg/mL at concentrations of 10-10^5 CFU/mL, whereas the G+ (*S. aureus* and GAS) had a much higher HAase productivity levels (4.8-12.6 mg/mL) at the same concentrations. These results were theoretically supported by the fingdings of Hu *et.al.* that a Glu-480 exists in the coding sequence of HAase, which is highly conserved in HAase from G+ compared to G- (Hu *et al.* 2022). Therefore, the different levels of bacterial HAase productivity could be used as an indicator to differentiate between G+ and G-. In addition, it has been reported that only live bacteria can produce HAase (Chen *et al.* 2023b), which allows us to distinguish between live and dead bacteria.

2.1.3 Optimization of HA Composite for the Linear Degradation by HAase

HA with different MW (1500-2500 kDa, 600 kDa, 40-100 kDa and 7 kDa) were selected to perform degradation by HAase. As shown in Fig. S1a, HA with a higher MW of 1500-2500 kDa had a significantly higher sensitivity ($p = 0.0038$) to HAase than the other groups, which could because of the greater number of glycosidic linkages in high MW HA resulted in higher binding affinity with HAase (Snetkov *et al.* 2020). It was also reported that the physicochemical properties and enzymolysis stability of HA composites depend on the volume ratios of high MW and low MW HA (Xue *et al.* 2020). Inspired by the study, HA with high MW (1500-2500 kDa) and low MW (7 kDa) were then composited at volume ratios of 8:1, 4:1, 2:1, 1:2, 1:4, and 1:8 to investigate their degradation rates by HAase. As shown in Fig. 1d, the HA composite with high MW and low MW of 8:1 was most sensitive to HAase and its degradation degree showed a strong linear relationship ($R^2 > 0.99$) with the concentration of HAase. This provides a clear mathematical relationship to allow quantitative detection to be obtained. The morphologies of above HA composites were characterized. Regardless of its MW,

HA was primarily characterized as having a "lamellar" structure and when high MW HA was combined with low MW HA, the microstructure exhibited the formation of "pore" and "fibrillary" structures (Fig. S1b). In addition, the HA composite with high MW and low MW at a ratio of 8:1 had a significantly higher density than the composites with other ratios regardless of changes in HA concentration (Fig. S1c).

2.1.4 Optimization and Characterization of CPRG-loaded HA Hydrogel as Bioreactor

A hydrogel-based bioreactor for the biosensor was prepared using HA composite (ratio of high MW to low MW = 8:1) as the main matrix and sodium alginate (SA) as the gellation assistant component (Guo *et al.* 2020). CPRG was first loaded in HA composite, followed by the addition of SA in the presence of Ca^{2+} to form the hydrogel bioreactor. As shown in Fig. S1d, a maximum CPRG loading efficiency of 92.1 ± 2.1% was achieved at a HA concentration of 3.0 wt%. At this concentration, the enzymatic properties exhibited by HA composite remained consistent with those described in section 2.1.3 (Fig. S1e).

The degradation behavior of the bioreactor by different types and concentrations of bacteria was invesitigated , as shown in Fig. 1e. An excellent linear correlation ($R^2 >$ 0.99) was found between the degree of degradation of the hydrogel and the concentrations of all tested bacteria. Two G+, which secreated more HAase, were capable of degrading over 85% of hydrogel at 10^5 CFU/mL, whereas two G- could only degrade less than 10% of the hydrogel at the same concentration. Additionally, the lowest degradation (18%) by G+ at 10 CFU/mL was still higher than that of the highest degradation (9%) of G- at 10^5 CFU/mL, confirming the capbility of this detection strategy to differentiate between G+ and G-.

The release profiles of CPRG from the bioreactor were also highly significantly linearly correlated ($R^2 > 0.99$) with the degradation of the hydrogel (Fig. 1f). In the case of G+ ranging in concentration from 10 to 10^5 CFU/mL, the released CPRG was between 28 to 200 μg/mL, whereas for G- at the same concentrations, the released CPRG was much lower in the range of 2 to 20 μg/mL. Collectively, there were notable linear correlations among the concentration of bacteria and the secreted HAase, the degradation of HA

hydrogel and the released CPRG. Therefore, the amount of released CPRG can be used as an indication of the initial concentration of bacteria.

2.1.5 Optimization and Characterization of β-gal-loaded Agar Hydrogel as Signal Generator

The optimal concentration of β-gal for the chromogenic reaction with CPRG was determined to be 20 μg/mL (section 2.1.1). The hydrogel selected to encapsulate β-gal was optimized to meet the following requirements. Firstly, the hydrogel should not be degradable by HAase to ensure all β-gal molecules would remain in the hydrogel and final output signal would only depend on the CPRG from bioreactor. Among all hydrogel candidates (agar, SA, and luria-bertani hydrogel shown in Fig. S2a), only the agar hydrogel released no β-gal in the presence or absence of HAase. (Fig. 1g, h and S2b) In addition, agar hydrogel itself was colorless and transparent,which did not interfere with the results of the chromogenic reaction bewteen β-gal and CPRG (Fig. S2a and Fig. 1i).

2.1.6 Optimization of Detection Parameters

The optimized reaction time between the biosensor and sample was determined in Fig. S3a-b, showing that the degradation reaction between HAase and HA hydrogel, as well as the color reaction between CPRG and β-gal, can both be completed within 30 min. Additionally, HAase exhibited maximum activity between 37-40°C and pH between 6-7.5 (Fig. S3c and f), while the catalysis of β-gal toCPRG was not affected by different temperatures or pH under our experimental settings (Fig. S3d, e, g and h). Thus, we selected 37°C and pH 7.4 for conducting enzymatic reactions in this study. Photographing conditions for obtaining detection results were optimized in Fig. S4, the color information was not affected by the distance between the smartphone camera and the signal generator, and as long as the phone flash was on, accurate color information can be obtained regardless of the light condition, indicating the compatibility of the biosensor. The images of signal generator can provide qualitative information about the presence/absence of bacteria using the naked eye (Fig. S5a). The semi-quantitative results of the type and concentration of bacteria can be achieved by substituting the RGB values of the image into our pre-constructed standard curves (Fig. S5b).

In the scenario for detecting a mixed sample of both G+ and G- bacteria, it was worth noting that firstly simultaneous infection of G+ and G- were uncommon in clinical settings due to their overlapping niches (Kuhn *et al.* 2022). Additionally, our results in Fig. S6 also demonstrated that when co-culturing G- (*P. aeruginosa*) and G+ (*S. aureus*) bacteria together, they cannot coexist, meaning there will be only one type of pathogenic bacteria in the final culture.

2.1.7 Determination of the LoD of Biosensor with Bacterial Standard Solutions in PBS and Serum

The LoD of this biosensor was determined using the G+ and G- standard solutions with PBS and serum as solvents. As shown in Fig. 1j, in PBS, the biosensor exhibited clear and sensitive color changes after the detection of bacteria and the colors gradually became saturated from light pink to deep rose with increasing bacterial concentration. Notably, differences in color changes for G+ and G- can easily be distinguished, since the color of the lowest concentration (10 CFU/mL) of G+ was even more saturated than that of the highest concentration (10^5 CFU/mL) of G-. Thus, we can obtain the LoD of this biosensor from the above results, which is calculated to be as low as 10 CFU/mL for both G+ and G-. Compared to other biosensors reported in major journals over the most recent years (Table S1), this biosensor excels in achieving a value of LoD of 10 CFU/mL without preprocessing of the sample or requirement of complex equipment. The detection time is controlled within 60 mins, which is applicable for daily uses. As shown in Fig. 1k, in serum, the biosensor can successfully detect and distinguish between G+ and G- with the resulting color changes displaying the similar trends as described above. However, compared to detection in PBS, the color of the signal generator presented a slight color shift due to the color of serum itself. Diluting colored samples with PBS before conducting the detection process could significantly reduced the impact of the original color of the sample on the result with the accuracy and sensitivity guaranteed and the optimal dilution factor was 2 (Fig. S7).

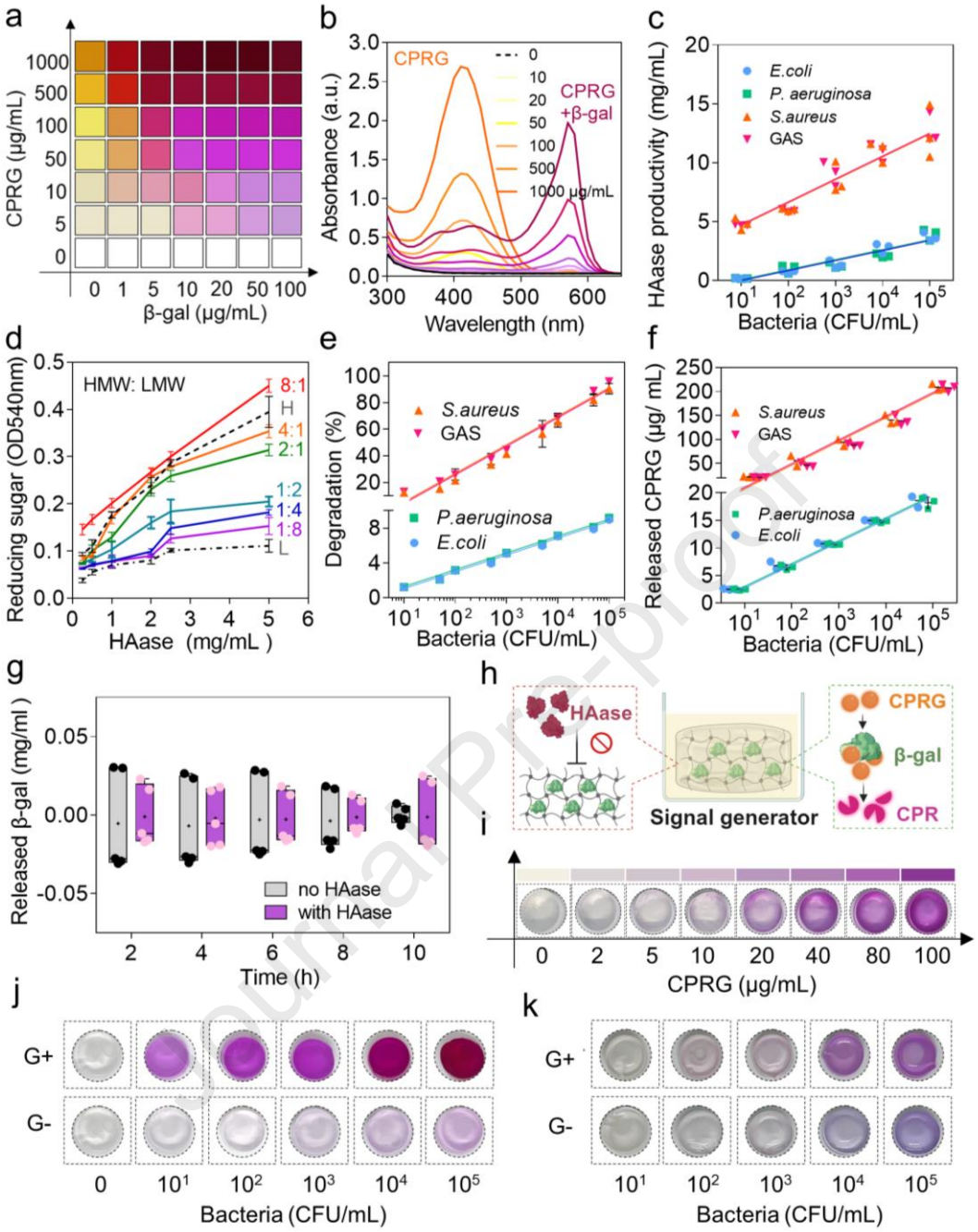

Fig. 1. Characterizations of the biosensor. (**a**) Analytical features of the color reaction between CPRG and β-gal. (**b**) Spectral change of CPRG with different concentration after incubation with β-gal (20 μg/mL). (**c**) The HAase productivity of different bacteria with different concentrations (10-10^5 CFU/mL). (**d**) Sensitivity of HA composite (2 mg/mL) prepared from high (1500-2500 kDa) and low (7 kDa) MW to HAase. (**e**) The degradation of HA hydrogel bioreactor with the different concentration (10-10^5 CFU/mL) and type (*S. aureus* and GAS as G+, *P. aeruginosa* and *E. coli* as G-) of bacteria. (**f**) The release of CPRG from bioreactor with the different concentration and type of bacteria. (**g**) The characterization and (**h**) reaction scheme of HAase non-

responsiveness of β-gal-loaded agar hydrogel signal generator. (**i**) Color-change effect of the β-gal-loaded agar hydrogel after react with different concentration of CPRG. (**j-k**) Detection results of different concentrations of bacterial solutions with (**j**) PBS or (**k**) 100% serum as solvent by this biosensor.

2.2 AI-assisted Smartphone Acquisition of Detection Results

The YOLOv5 algorithm was used for the precise analysis of the results obtained by the biosensor in this study. As shown in Fig. 2a and S8, YOLOv5 is composed of backbone, neck, and head (Chen *et al.* 2023a). The backbone utilizes the Cross-Stage Partial (CSP) network strategy in the CSP-Darknet53 convolutional network. The neck integrates the Bottle Neck CSP into the Path Aggregation Network and incorporates a variation of the Spatial Pyramid Pooling (SPP). The head consists of three convolution layers which predict the coordinates of the bounding box, scores, and classes of objects (Chen *et al.* 2023a).

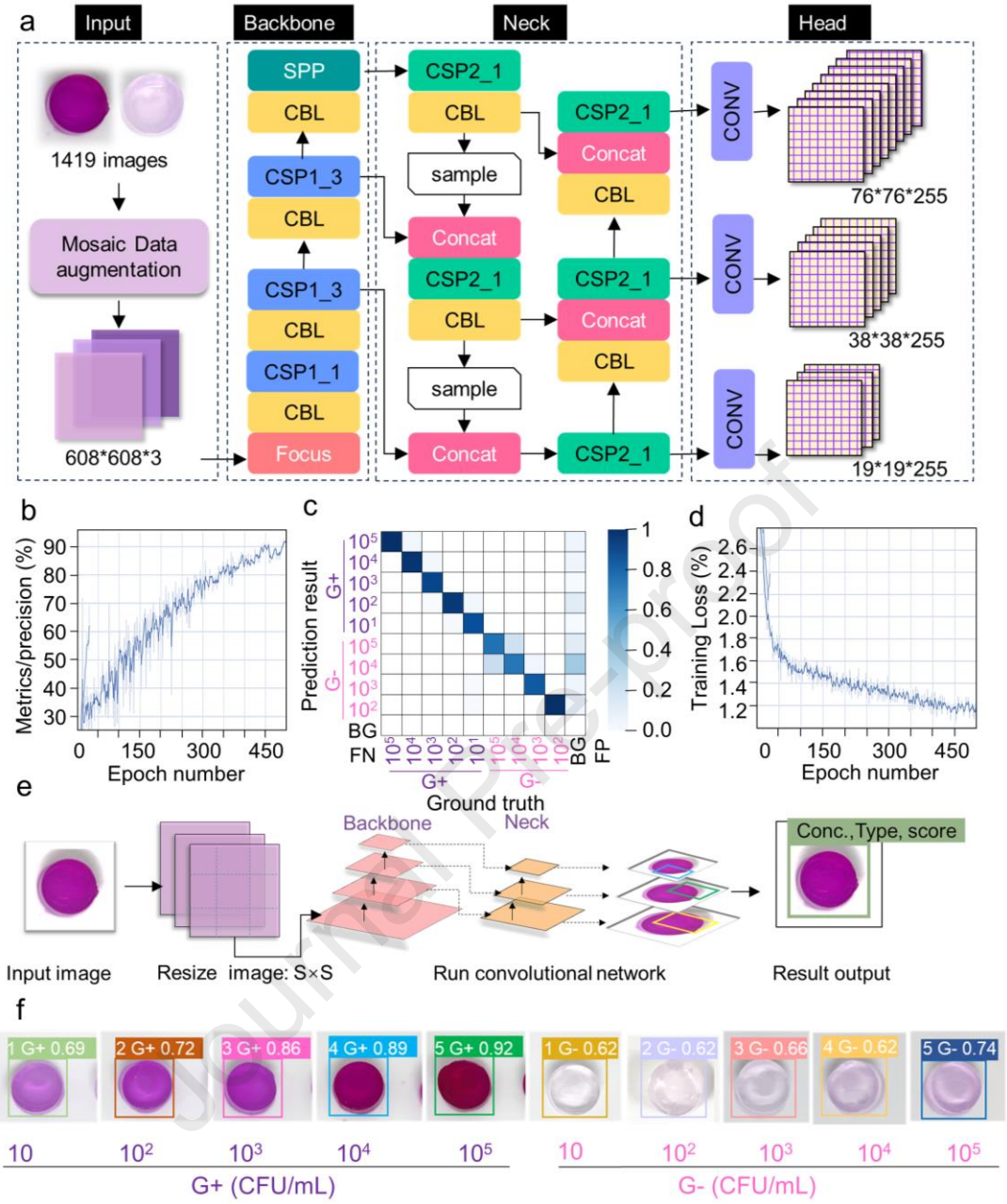

Fig. 2. AI-assisted acquisition of the detection results. (**a**) YOLOv5 network architecture. (**b**) The precision of YOLOv5. (**c**) The confusion matrix of the verification results for the 10 categories of perspiration. BGFN: background false negatives, BGFP: background false positives. (**d**) The training loss of YOLOv5. (**e**) YOLOv5 algorithm flowchart. (**f**) Example of detection result output.

In this study, 1419 images from the signal generator were used to train YOLOv5. After 500 epochs, the detection accuracy reached 92% (Fig. 2b and 2c) and the training loss decreased to 1.2% (Fig. 2d). When analyzing the input image, bounding boxes were generated using three featured maps based on the parameters optimized during the

training phase (Fig. 2e). The illustrative output was shown in Fig. 2f. The results were consisted three parts: the log value of the concentration of bacteria detected, followed by the bacterial type (G+ and G-) and the confidence level. In general, higher confidence levels indicate more accurate results, however, a low confidence level does not mean that the output is not credible, since the algorithm will not output any results when the detection results are not credible. To summarize, the use of the YOLOv5 algorithm enables rapid and accurate bacterial detection, with the potential for future integration across various terminals and platforms.

2.3 Application in Detection of Live Bacteria

The biosensor proposed in the present work detects the HAase produced by live bacteria, avoiding the limitations of bacterial culturability and interference of dead bacteria and its application in detection of live bacteria was demonstrated. Live and dead bacterial solutions (*E. coli* as G-, *S. aureus* as G+) were prepared by mixing them at different ratios (100%-20%) for further detection (Fig. 3a). The results were shown in Fig. 3b. The significance of the results may not be obvious to the naked eye, given that the concentration of live bacteria in mixed bacterial samples were all at the same order of magnitude (10^4 CFU/mL). However, the use of computer vision techniques means that information such as the grey value of these signal generator colors could be analyzed (Fig. 3b), which provides detection results with higher accuracy (Fig. 3c). In summary, the proposed biosensor can correctly detect the proportion of live bacteria in a mixture of live and dead bacteria, confirming the potential application of the biosensor in the above field.

2.4 Application in Detecting Bacteria in Food Samples

We demonstrated the application of the biosensor for detecting bacteria in food samples as shown in Fig. 3d. Our biosensor reported that higher concentrations of bacteria solution used to contaminate the blueberries led to higher levels of bacteria detected on the blueberries as shown in 3e. This finding was supported by the results of the culture method (Fig. 3d). The concentration of bacteria subsequently detected on blueberries was not consistent with the concentration of bacteria that incipiently contaminated the sterile blueberries, which may be because not all bacteria were able to attach to the blueberries and the proliferative behavior of the bacteria was unpredictable.

Nevertheless, the biosensor provides a reference for on-site quality control in food production enterprises, rapid quality inspection for food safety, and quality control for consumers prior to consuming food.

2.5 Application in Antimicrobial Susceptibility Testing (AST)

The application of the biosensor in AST was demonstrated. Penicillin-streptomycin solutions with different concentrations (0-10 mg/mL) were co-incubated with four typical bacteria (*E. coli, P. aeruginosa, S. aureus* and Methicillin-resistant *Staphylococcus aureus* (MRSA)) followed by detecting the concentration of remaining live bacteria with the proposed biosensors. Bacterial susceptibility to an antibiotic is assessed in term of the ratio of the concentrations of dead to total bacteria (10^5 CFU/mL). The results showed that *S. aureus, E. coli,* and MRSA had a susceptibility rate of 99% to the antibiotic at a concentration of 0.6 mg/mL (Fig. 3f-g). However, *P. aeruginosa* only became susceptible to the antibiotic at a concentration of 10 mg/mL. The results of the dilution method showed the similar conclusion that *E. coli, S. aureus* and MRSA were sensitive strains while *P. aeruginosa* exhibited drug resistance to the antibiotic (Fig. 3f and S9). This means that our biosensor has a 0% serious error rate (misidentification as a sensitive strains) and 0% major error rate (misidentification as a drug-resistant strains) when performing AST, complying with the Food and Drug Administration (FDA) requirements (the rate of serious errors < 1.5% and that of major errors < 3.0%). In summary, our biosensor is rapid, simple and effective for AST applications.

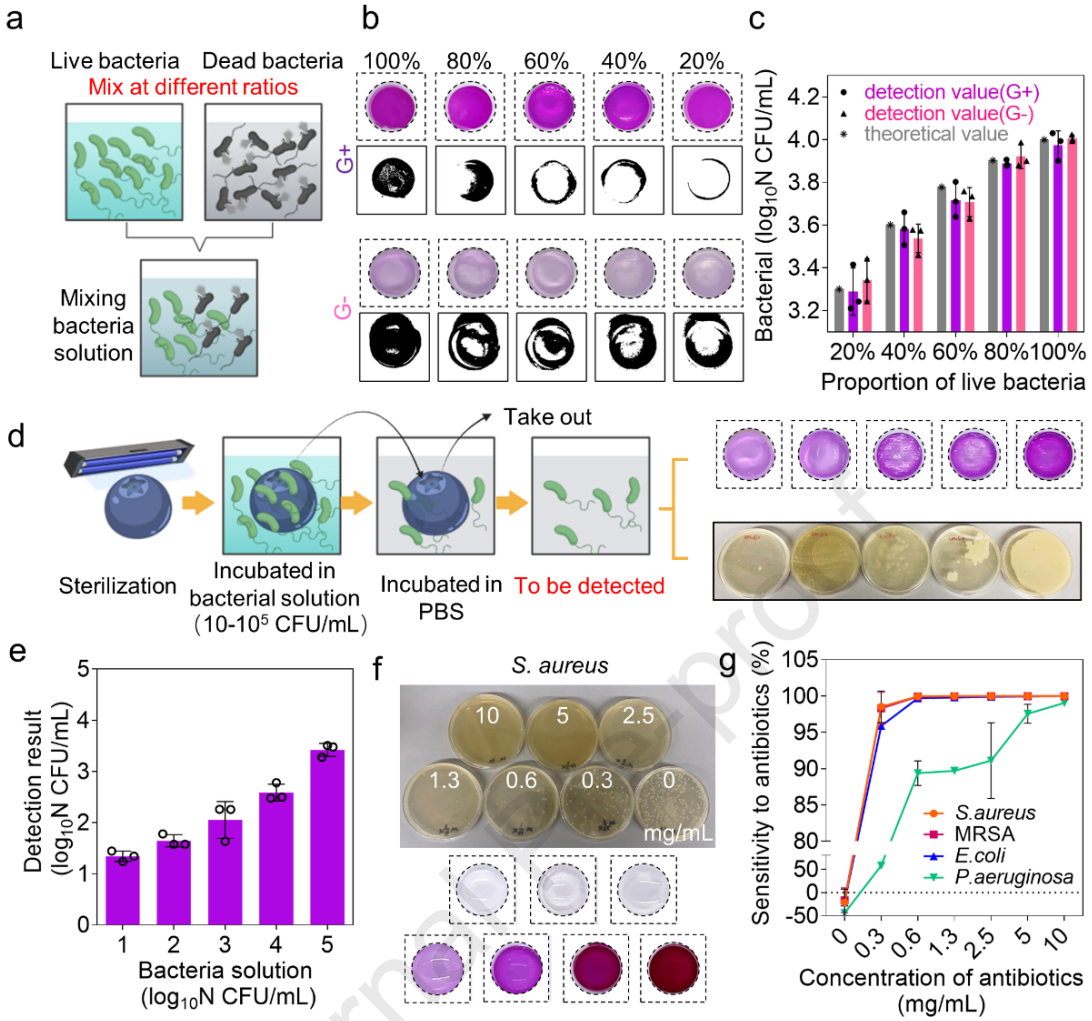

Fig. 3. Application of the biosensor in (**a-c**) detection of live bacteria. (**a**) Preparation of bacteria solutions with different percentage (20%-100%) of live bacteria (10^4 CFU/mL). (**b**) Image results produced by the biosensor. Greyscale mode of these images also displayed, which is a categorization prediction basis parameter in the machine learning process. (**c**) Quantitative results produced by this biosensor. (**d-e**) Detection bacteria in food samples. (**d**) Preparation of bacterially contaminated food model (blueberry) and the detection results produced by our biosensor and the culture method, respectively. (**e**) Quantitative results produced by this biosensor. (**f-g**) Application in antimicrobial susceptibility testing. (**f**) The image results of the detection produced by our biosensor and the culture method, respectively. (**g**) Quantitative results produced by this biosensor.

2.6 Evaluation Bacterial Infection from Clinical Samples

To determine the potential of the proposed biosensor for clinical applications, we collected 12 samples from abscesses and detected them by the biosensor with analysis using YOLOv5 (Fig. 4a). Furthermore, empirical diagnosis from doctor and culture method were used as two independent methods to verify the accuracy of this biosensor (Table 1). Our biosensor showed 8 G+ and 4 G- infections (Fig. 4b and 4c, purple bar) in all samples. Meanwhile, the report issued by the hospital laboratory indicated that 8 out of the 12 samples were "confirmed bacterial infection" (6 G+ and 2 G-, Fig. 4b and 4c, orange bar) and 4 were "undetermined bacterial infection". However, in the clinical situation, all 4 patients had obvious signs of infection with the presence of an abscess at the site of the lesion and doctors implemented anti-infection treatment based on experience. Briefly, as shown in Table 1, case No.1 and 3 recovered within one week after treatment. Antibiotics were not prescribed for case No.9, who returned to the hospital after 19 days. Notably, for case No.10, a relative longer period of treatment (35 days) was required despite no indication of infection in the gold standard report. An antibiotic specifically targets G+ was prescribed, while our biosensor results indicated that the patient was infected with G-, which may explain the patient's failure to recover.

Receiver operating characteristic curves were developed to evaluate the clinical sensitivity and specificity of our biosensor, and those were compared with those for the culture method. Both the sensitivity and specificity of our biosensor were found to be 100% (Fig. 4d). Meanwhile, the clinical sensitivity for the culture method was determined to be only 67.7 %, along with 100% clinical specificity. These results further confirmed that our biosensor has potential values to satisfy clinical needs. Therefore, our biosensor is applicable to assist the docotors to make more precise diagnosis and prescribe more appropriate treatment for patients.

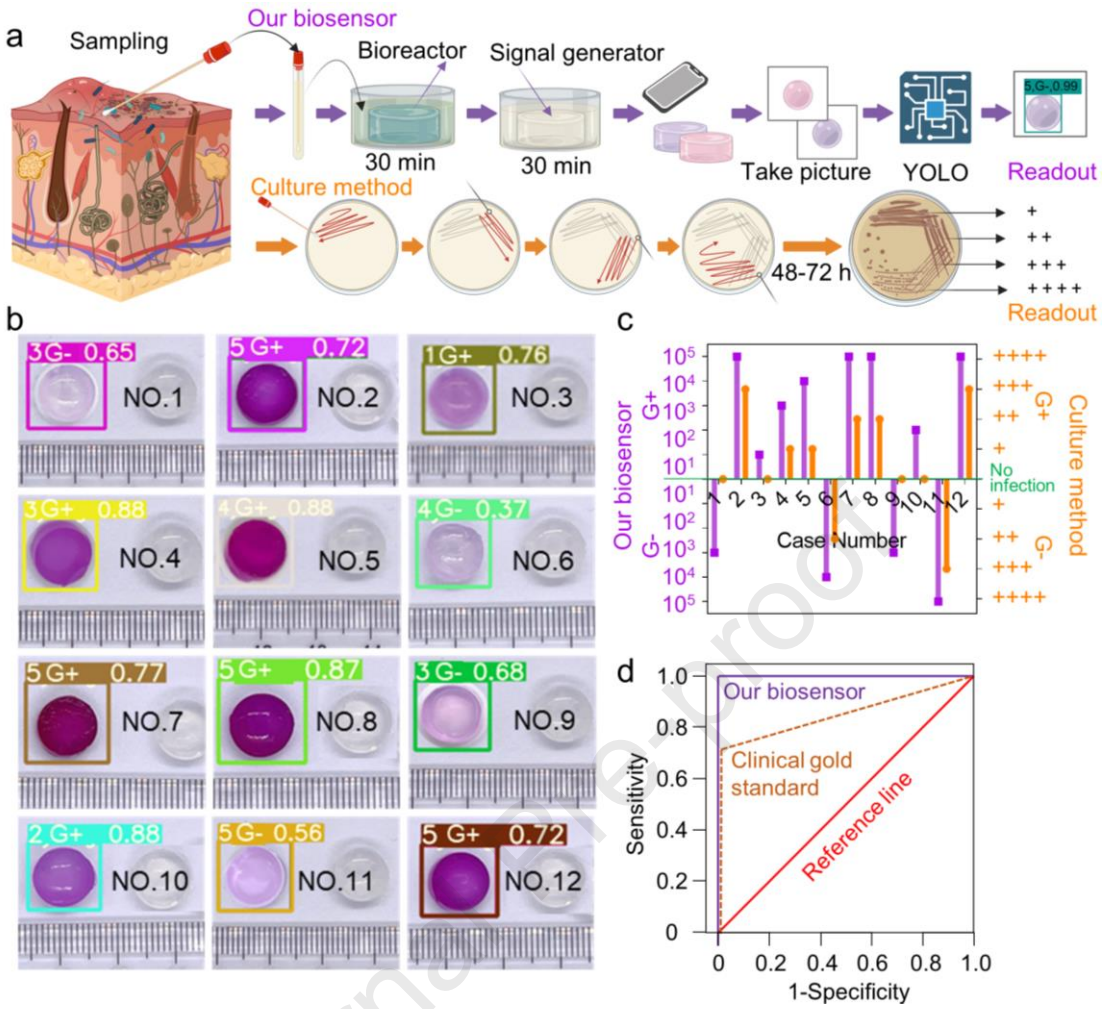

Fig. 4. Detection of bacteria in the clinical samples. (**a**) Operation flow of this biosensor and culture method for the detection of bacteria in clinical samples, respectively. (**b**) 12 samples detected by the biosensor and the results output obtained by the YOLOv5 algorithm. (**c**) Results obtained by our biosensor and culture method, respectively. The green horizontal coordinate in the graph indicates "no bacterial infection". (**d**) Receiver operating characteristic curves of our biosensor and culture method.

Table 1. Clinical information for the abscess and empyema samples.

Gold standard	Our biosensor	Symptom	Doctors' diagnosis	Treatment /Medication	Course (day)	NO.
Negative	G-, 10^3	Furuncle (head)	Infection	IDA+CPHDT	5	1
Negative	G+, 10	Furuncle (head)	Infection	IDA+CPHDT	>6	3
Negative	G-, 10^3	Epidermoid cyst	Infection	IDA	19	9
Negative	G+, 10^2	Keloid	Infection	IDA+MOM	>35	10
G+, +++	G+, 10^5	Furuncle (limb)	Infection	IDA	>11	2
G+, +++	G+, 10^5	Acute paronychia	Infection	IDA+CAT	/	12
G+, ++	G+, 10^5	Abscess (head)	Infection	IDA+CDS	12	7
G+, ++	G+, 10^5	Furuncle (trunk)	Infection	BB	/	8
G+, +	G+, 10^3	Cyst (trunk)	Infection	IDA+CAT	>20	4
G+, +	G+, 10^4	Sebaceous gland cyst	Infection	IDA+CAT	/	5
G-, +++	G-, 10^5	Ulcer dermatitis	Infection	DT+MOM	>37	11
G-, ++	G-, 10^4	Folliculitis (head)	Infection	DHT	>25	6

IDA: incision and drainage of abscess; DT: debridement therapy; CPHDT: clindamycin palmitate hydrochloride dispersible tablets; CAT: cefuroxime axetil tablets; DHT: doxycycline hyclate tablets; CDS: Cefaclor dry suspension; BB: benzathine benzylpenicillin for injection; MOM: mupirocin oint ment

3. Conclusion

This work provided an AI-assisted smartphone-based colorimetric biosensor for the point-of-care detection of pathogenic bacteria producing HAase, which achieved a LoD of 10 CFU/mL in 60 mins and was able to differentiate between types and concentrations of bacteria in both PBS and serum. The results were obtained from the analysis of color signals using a self-developed YOLOv5 algorithm, which provided high identification accuracy (> 92%). The biosensor showed its superior performance in detecting bacteria in food samples, performing antimicrobial susceptibility testing and assessing bacterial infections in clinical cases, showing promising and broad application potential.

References

AbdElFatah, T., Jalali, M., Yedire, S.G., I. Hosseini, I., del Real Mata, C., Khan, H., Hamidi, S.V., Jeanne, O., Siavash Moakhar, R., McLean, M., Patel, D., Wang, Z., McKay, G., Yousefi, M., Nguyen, D., Vidal, S.M., Liang, C., Mahshid, S., 2023. Nature Nanotechnology 18(8), 922-932.http://doi.org/10.1038/s41565-023-01384-5

Chen, H., Xu, S., Liu, H., Liu, C., Liu, H., Chen, J., Huang, H., Gong, H., Wu, J., Tang, H., Luo, J., Wen, B., Zhou, J., Qiao, Y., 2023a. Advanced Functional Materials.http://doi.org/10.1002/adfm.202309798

Chen, J., Su, Y., Huo, J., Zhou, Q., Li, P., 2023b. Colloid and Interface Science Communications 57.http://doi.org/10.1016/j.colcom.2023.100752

Creran, B., Li, X., Duncan, B., Kim, C.S., Moyano, D.F., Rotello, V.M., 2014. ACS Applied Materials & Interfaces 6(22), 19525-19530.http://doi.org/10.1021/am505689g

Dsouza, A., Constantinidou, C., Arvanitis, T.N., Haddleton, D.M., Charmet, J., Hand, R.A., 2022. ACS Applied Materials & Interfaces 14(42), 47323-47344.http://doi.org/10.1021/acsami.2c08582

Flachot, A., Gegenfurtner, K.R., 2021. Vision Research 182, 89-100.http://doi.org/10.1016/j.visres.2020.09.010

Gui, Y., Zeng, Y., Chen, B., Yang, Y., Ma, J., Li, C., 2023. Nature Communications 14(1).http://doi.org/10.1038/s41467-023-38733-w

Guo, X., Wang, Y., Qin, Y., Shen, P., Peng, Q., 2020. International Journal of Biological Macromolecules 162, 618-628.http://doi.org/10.1016/j.ijbiomac.2020.06.180

Hu, H., Liu, H., Kweon, O., Hart, M.E., 2022. Canadian Journal of Microbiology 68(1), 31-43.http://doi.org/10.1139/cjm-2021-0110

Kuhn, T., Mamin, M., Bindschedler, S., Bshary, R., Estoppey, A., Gonzalez, D., Palmieri, F., Junier, P., Richter, X.L., 2022. R Soc Open Sci 9(12), 211592.http://doi.org/10.1098/rsos.211592

Liu, X., Kukkar, D., Deng, Z., Yang, D., Wang, J., Kim, K.H., Zhang, D., 2023. Biosens Bioelectron 235, 115317.http://doi.org/10.1016/j.bios.2023.115317

Meng, Z., Xu, S., Wang, L., Gong, Y., Zhang, X., Zhao, Y., 2022. Energy Science & Engineering 10(3), 800-813.http://doi.org/10.1002/ese3.1056

Mi, F., Hu, C., Wang, Y., Wang, L., Peng, F., Geng, P., Guan, M., 2022. Analytical and Bioanalytical Chemistry 414(9), 2883-2902.http://doi.org/10.1007/s00216-021-03872-w

Mohammed, M., Devnarain, N., Elhassan, E., Govender, T., 2022. WIREs Nanomedicine and Nanobiotechnology 14(4).http://doi.org/10.1002/wnan.1799

Nißler, R., Bader, O., Dohmen, M., Walter, S.G., Noll, C., Selvaggio, G., Groß, U., Kruss, S., 2020. Nature Communications 11(1).http://doi.org/10.1038/s41467-020-19718-5

Petrucci, S., Costa, C., Broyles, D., Dikici, E., Daunert, S., Deo, S., 2021. Trends in Food Science & Technology 115, 409-421.http://doi.org/10.1016/j.tifs.2021.06.054

Rentzsch, R., Deneke, C., Nitsche, A., Renard, B.Y., 2020. Briefings in Bioinformatics 21(5), 1596-1608.http://doi.org/10.1093/bib/bbz076

Shenashen, M.A., Emran, M.Y., El Sabagh, A., Selim, M.M., Elmarakbi, A., El-Safty, S.A., 2022. Progress in Materials Science 124.http://doi.org/10.1016/j.pmatsci.2021.100866

Snetkov, P., Zakharova, K., Morozkina, S., Olekhnovich, R., Uspenskaya, M., 2020. Polymers 12(8).http://doi.org/10.3390/polym12081800

Xu, L., Ramadan, S., Akingbade, O.E., Zhang, Y., Alodan, S., Graham, N., Zimmerman, K.A., Torres, E., Heslegrave, A., Petrov, P.K., Zetterberg, H., Sharp, D.J., Klein, N., Li, B., 2021. ACS Sensors 7(1), 253-262.http://doi.org/10.1021/acssensors.1c02232

Xue, Y., Chen, H., Xu, C., Yu, D., Xu, H., Hu, Y., 2020. RSC Advances 10(12), 7206-7213.http://doi.org/10.1039/c9ra09271d

Zamboni, F., Wong, C.K., Collins, M.N., 2023. Bioactive Materials 19, 458-473.http://doi.org/10.1016/j.bioactmat.2022.04.023

Zhang, Z., Sun, Y., Yang, Y., Yang, X., Wang, H., Yun, Y., Pan, X., Lian, Z., Kuzmin, A., Ponkratova, E., Mikhailova, J., Xie, Z., Chen, X., Pan, Q., Chen, B., Xie, H., Wu, T., Chen, S., Chi, J., Liu, F., Zuev, D., Su, M., Song, Y., 2023. Adv Mater 35(12),

e2211363.http://doi.org/10.1002/adma.202211363

Data availability

Data will be made available in supplementary information.

CRediT authorship contribution statement

Rongwei Cui: Conceptualization; Data curation; Formal analysis; Methodology; Software; Writing – original draft; Writing – review & editing. **Huijing Tang**: Resources; Methodology; Software; Writing – original draft; Writing – review & editing. **Qing Huang**: Methodology; Software; Writing – original draft; Writing – review & editing. **Tingsong Ye**: Data curation; Writing – review & editing. **Jiyang Chen:** Data curation; Formal analysis. **Yinshen Huang**: Methodology; Software. **Chongchao Hou**: Resources; Formal analysis. **Sihua Wang:** Resources; Formal analysis. **Sami Ramadan:** Investigation; Writing – review & editing. **Bing Li:** Investigation; Writing – review & editing. **Yunsheng Xu:** Resources; Writing – review & editing. **Lizhou Xu:** Conceptualization; Formal analysis; Investigation; Methodology; Supervision; Writing – review & editing. **Danyang Li:** Conceptualization; Formal analysis; Funding acquisition; Investigation; Methodology; Project administration; Resources; Supervision; Writing – original draft; Writing – review & editing.

Declaration of competing interest

Danyang Li has a patent licensed to The Seventh Affiliated Hospital of Sun Yat-sen University.

Acknowledgements

This work is supported by National Natural Science Foundation of China (Grant Nos. 52103198, 52311530079 and 32301683), Basic and Applied Basic Research Foundation of Guangdong Province (2023A1515010067), Zhejiang Provincial Natural Science Foundation of China (No. LR23C130001), Science, Technology and Innovation Commission of Shenzhen Municipality (RCBS20210609104333005 and JCYJ20220530145001003).

We thank Dr. Xiao-Yong Zhan for providing bacteria, and the Dermatology, the Laboratory Departments and the Biobank of the Seventh Affiliated Hospital of Sun

503 Yat-sen University for helping in clinical sample collection and the bacterial culture
504 study.

Table 1. Clinical information for the abscess and empyema samples.

Gold standard	Report time (day)	Our biosensor	Clinical manifestation	doctors' diagnoses	Treatment Medication	Course (day)	NO.
Negetive	3	G-, 10^3	Furuncle (head)	Infetion	IDA+CPHDT	5	1
Negetive	2	G+, 10	Furuncle (head)	Infection	IDA+CPHDT	>6	3
Negetive	2	G-, 10^3	epidermoid cyst	Infection	IDA	19	9
Negetive	2	G+, 10^2	keloid	Infection	IDA+MOM	>35	10
G+, +++	3	G+, 10^5	Furuncle (lower limb)	Infection	IDA	>11	2
G+,+++	3	G+, 10^5	Acute paronychia	Infection	IDA+CAT	/	12
G+, ++	3	G+, 10^5	Abscess (head)	Infection	IDA+CDS	12	7
G+, ++	3	G+, 10^5	Furuncle (runk)	Infection	BB	/	8
G+, +	2	G+, 10^3	Cyst (runk)	Infection	IDA+CAT	>20	4
G+, +	3	G+, 10^4	Sebaceous gland cyst	Infection	IDA+CAT	/	5
G-, +++	3	G-, 10^5	Ulcer dermatitis	Infection	DT+MOM	>37	11
G-, ++	3	G-, 10^4	Folliculitis (head)	Infection	DHT	>25	6

DA: incision and drainage of abscess; DT: debridement therapy; CPHDT: clindamycin palmitate hydrochloride dispersible tablets; CAT: cefuroxime axetil tablets; DHT: doxycycline hyclate tablets; CDS: Cefaclor dry suspension; BB: benzathine benzylpenicillin for injection; MOM: mupirocin oint ment

Declaration of interests

☐ The authors declare that they have no known competing financial interests or personal relationships that could have appeared to influence the work reported in this paper.

☒The authors declare the following financial interests/personal relationships which may be considered as potential competing interests:

Danyang Li has a patent licensed to the Seventh Affiliated Hospital of Sun Yat-sen University.